JACS
JOURNAL OF THE AMERICAN CHEMICAL SOCIETY
pubs.acs.org/JACS
Communication

Phase Separation Modulates the Thermodynamics and Kinetics of RNA Hybridization

Atul K. Rangadurai,* Lisa Ruetz, Rashik Ahmed, Kristen Lo, Martin Tollinger, Julie D. Forman-Kay, Christoph Kreutz, and Lewis E. Kay*

Cite This: J. Am. Chem. Soc. 2024, 146, 19686−19689
Read Online
ACCESS | Metrics & More | Article Recommendations | Supporting Information

ABSTRACT: Biomolecular condensates can influence cellular function in a number of ways, including by changing the structural dynamics and conformational equilibria of the molecules partitioned within them. Here we use methyl transverse relaxation optimized spectroscopy (methyl-TROSY) NMR in conjunction with 2′-*O*-methyl labeling of RNA to characterize the thermodynamics and kinetics of RNA−RNA base pairing in condensates formed by the C-terminal intrinsically disordered region of CAPRIN1, an RNA-binding protein involved in RNA transport, translation, and stability. CAPRIN1 condensates destabilize RNA−RNA base pairing, resulting from a ∼270-fold decrease and a concomitant ∼15-fold increase in the on- and off-rates for duplex formation, respectively. The ∼30-fold slower diffusion of RNA single strands within the condensed phase partially accounts for the reduced on-rate, but the further ∼9-fold reduction likely reflects shedding of CAPRIN1 chains that are interacting with the RNA prior to hybridization. Our study emphasizes the important role of protein solvation in modulating nucleic acid recognition processes inside condensates.

Biomolecular phase separation, a process by which proteins, nucleic acids, and metabolites are concentrated to form condensates in the absence of an enclosing lipid membrane, plays an important role in modulating cellular function.[1] Ribonucleoprotein (RNP) granules are biomolecular condensates composed of RNAs and proteins that are involved in key aspects of RNA metabolism such as its processing, translation, stability, and transport.[2] Mutations in proteins and RNA molecules comprising RNP granules that alter their propensity to form condensates play a role in a variety of neurodegenerative and neurodevelopmental diseases.[3,4] Characterizing the structure and dynamics of RNA and protein molecules in these condensates is key to understanding RNP granule function and the structural transitions underlying the formation of aberrant condensates in disease. It has been shown that condensates can alter the secondary[5] and tertiary structures[6] and the unfolding energetics of RNA molecules,[6,7] as well as the catalytic activities of RNA enzymes.[8] Nevertheless, the kinetics of RNA folding transitions and the unique role that solvation by proteinaceous components within condensates plays in controlling RNA recognition processes have not been quantified.

Solution NMR spectroscopy is well suited for atomic resolution studies of RNA molecules in liquid-like condensates as long as experiments are designed to minimize signal losses due to spin relaxation and to mitigate the large dynamic range issues associated with studies of RNA molecules at low concentrations (∼1 mM; "client") in highly concentrated protein environments (∼20−30 mM; "scaffold").[9] Motivated by successes in the protein NMR field with using methyl groups as reporters of structure and dynamics in high molecular weight protein complexes,[10] we sought to use these probes in the present study focusing on RNA. As most RNA molecules do not contain methyl groups, we chose to add a 2′-*O*-methyl group probe, a naturally occurring post-transcriptional modification.[11] Our choice was motivated by studies showing that single 2′-*O*-methyl groups minimally perturb the thermodynamics of RNA base pairing[12] (stabilization by <0.3 kcal/mol) and the fact that the resonance positions of such groups (∼3.5 ppm and ∼60 ppm in ^{1}H and ^{13}C, respectively) are isolated from peaks derived from the protein scaffold.

Here we have used condensates formed from the last 103 residues of the C-terminal intrinsically disordered region of CAPRIN1 (henceforth referred to as CAPRIN1), an RNA binding protein found in P-bodies, and stress and transport granules,[13,14] which are integral for RNA processing, translational regulation, and transport.[2] An RNA duplex has been chosen as a client, as duplexes are ubiquitous and functional elements of RNA structure. A single guanosine residue in the middle of the helix was modified with a 2′-*O*-methyl group with ^{13}C labeling, as a probe of RNA structural dynamics in the condensed phase (Figure 1A). The 2′-*O*-methyl ^{1}H and ^{13}C chemical shifts are sensitive to RNA hybridization due to changes in sugar puckering upon base pairing.[15]

Condensed-phase NMR samples containing CAPRIN1 and RNA were prepared as described in Supporting Information (Figure S1), with equimolar amounts of the two comple-

Received: May 13, 2024
Revised: July 2, 2024
Accepted: July 3, 2024
Published: July 11, 2024

https://doi.org/10.1021/jacs.4c06530
J. Am. Chem. Soc. 2024, 146, 19686−19689

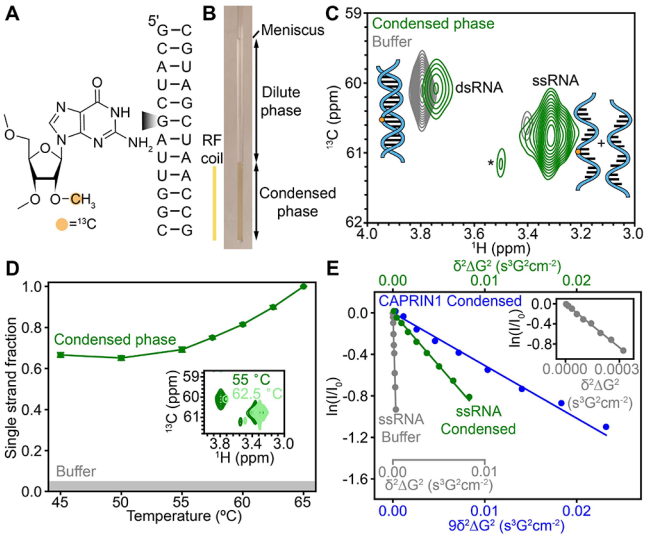

Figure 1. (A) Secondary structure of the RNA duplex used in this study, with a 2′-*O*-methyl modification at the indicated guanosine. The methyl group is ^{13}C labeled. (B) 3 mm tube containing the phase-separated sample used for NMR measurements. (C) Overlay of [^{13}C,^{1}H] ddHMQC spectra of the RNA methyl region of the condensed phase (green) and buffer (gray; plotted at a low level so that the ssRNA peak is visible) samples, 57.5 °C, 800 MHz, recorded under identical conditions, along with schematic representations of the RNA in dsRNA and ssRNA states. * denotes a minor peak arising from weak interactions between the single strand and duplex (Figure S3). (D) Variation of the ssRNA fraction in the condensed phase with temperature (green). The gray region denotes the maximum fraction of ssRNA in buffer (65 °C) with a total RNA concentration as in the condensed phase (Supporting Information). (Inset) Overlay of [^{13}C,^{1}H] ddHMQC spectra of the RNA methyl region of the condensed phase sample at 55 and 62.5 °C. (E) Normalized intensities (points) of methyl signals in pulsed field gradient diffusion experiments, for ssRNA in buffer (gray) and condensed phase (green) and for CAPRIN1 in the condensed phase (blue), 57.5 °C. δ and Δ are total time for bipolar defocusing/refocusing gradient pairs and the diffusion time used in the measurements, respectively (Supporting Information). Solid lines are fits to extract diffusion coefficients. (Inset) Zoomed-in view of the data for the ssRNA in buffer. All measurements were performed in 10 mM sodium phosphate, 200 mM NaCl, pH 7.0, 10% D_2O; the RNA concentration was 100 μM (950 μM) for each strand for measurements in buffer (condensate), with the exception of the ssRNA buffer sample in E (gray), where 25 μM RNA concentration was used.

mentary RNA strands of the helix added, both shown to partition into the condensate similarly (Supporting Information and Figure S2). As the condensed phase in the 3 mm NMR sample tube covers the radio frequency coil (Figure 1B), only the condensed phase signals are measured in the NMR experiments. Delayed decoupling heteronuclear multiple quantum coherence (ddHMQC) experiments, which take advantage of a methyl TROSY effect,[16] were recorded, using pulsed field gradients for coherence transfer selection to eliminate noise from natural abundance CAPRIN1 signals.[9] Spectra of the RNA in buffer (Figure 1C, gray: 100 μM of each RNA strand, 200 mM NaCl) show peaks for both the duplex (dsRNA) and single-stranded (ssRNA) forms of the RNA, with dsRNA the predominant species at 57.5 °C. In contrast, the ssRNA is dominant in the condensed phase (Figure 1C, green: ~1 mM of each RNA strand, 200 mM NaCl) at the same temperature, indicating destabilization of the duplex RNA, as has also been described previously for nucleic acids in other condensates.[6,7] In addition, there is a minor peak (*) arising from interaction of the single-stranded species with the duplex (Figure S3), which has not been considered in subsequent analyses, as it is only ~2% of the major ssRNA peak. Destabilization of dsRNA is also evident in temperature-dependent measurements in which the RNA is completely single stranded in the condensed phase at 65 °C, while only a minor fraction is melted in buffer at this temperature and concentration (<5%) (Figure 1D, Supporting Information).

We used pulse field gradient based NMR measurements (Supporting Information) to quantify the translational diffusion rates of ssRNA and CAPRIN1 in the CAPRIN1 condensate (Figure 1E). As expected, based on its smaller size (3 kDa vs 11 kDa), the ssRNA diffuses faster (D = (14.3 ± 0.4) × 10^{-8} cm^2/s) than CAPRIN1 (D = (7.1 ± 0.3) × 10^{-8} cm^2/s) by 2-fold in the condensate, but ~30-fold slower than in buffer (D = (40.7 ± 1.0) × 10^{-7} cm^2/s). Notably, the signal from the dsRNA could not be observed in the measurements in the condensed phase, due to rapid signal loss during the relatively insensitive diffusion experiment.

To explore the kinetic origins of the destabilization of dsRNA in the CAPRIN1 condensed phase relative to buffer, we recorded magnetization exchange experiments as a function of exchange time (T), to quantify the on- (k_{on}) and off- (k_{off}) rates of duplex formation,[17] and interpreted the resulting time-dependent signal intensities in terms of a two-state exchange model[18] (Figure 2A). Magnetization exchange experiments are typically performed by recording intensities of cross- and diagonal-peaks in experiments where the exchange block (T) is placed after the heteronuclear (in this case carbon) chemical shift evolution period (Figure S4 and Supporting Information).[17] However, the 2′-*O*-methyl ^{13}C chemical shifts of ssRNA and dsRNA are not sufficiently resolved to allow for accurate quantitation of the resulting cross-peaks (Figure S4). This situation is exacerbated by the fact that the exchange rates are close to an order of magnitude smaller than the intrinsic decay of the dsRNA signal, attenuating the buildup of cross-peak intensities (Supporting Information, Table S1). Here we use an alternative approach whereby the T-evolution of the diagonal-peaks, recorded in pairs of experiments where the exchange block is placed either before or after the ^{13}C evolution period (Supporting Information, Figures S5 and S6), is analyzed. The robustness of the approach has been validated (Figure S7), and cross-relaxation of the 2′-*O*-methyl group with adjacent protons is shown to have little effect on the extracted rates (Supporting Information and Figure S8).

The diagonal peaks from the exchange data recorded in this manner could be fit to extract k_{on} and k_{off} rates for duplex hybridization of 810 ± 120 M^{-1} s^{-1} and 2.9 ± 0.4 s^{-1} at 57.5 °C, respectively (Supporting Information, Figures 2B and C) in the condensed phase, with corresponding rates for RNA in buffer with the same bulk NaCl concentration (200 mM) of k_{on} = (2.2 ± 0.5) × 10^5 M^{-1} s^{-1} and k_{off} = 0.2 ± 0.1 s^{-1} (Figures 2B and C, Tables S1 and S2). Thus, the high concentration of CAPRIN1 in the condensed phase leads to a decrease in k_{on} by ~270-fold and an increase in k_{off} by ~15-fold relative to buffer (Figure 2C). The decrease in diffusion rate for ssRNA in the condensed phase (Figure 1E) can only account for ~30-fold of the ~270-fold relative decrease in k_{on}, with the remaining ~9-fold attenuation likely resulting from the requirement for removal of CAPRIN1 molecules associated with each single strand prior to hybridization. Similarly, the 15-

https://doi.org/10.1021/jacs.4c06530
J. Am. Chem. Soc. 2024, 146, 19686−19689

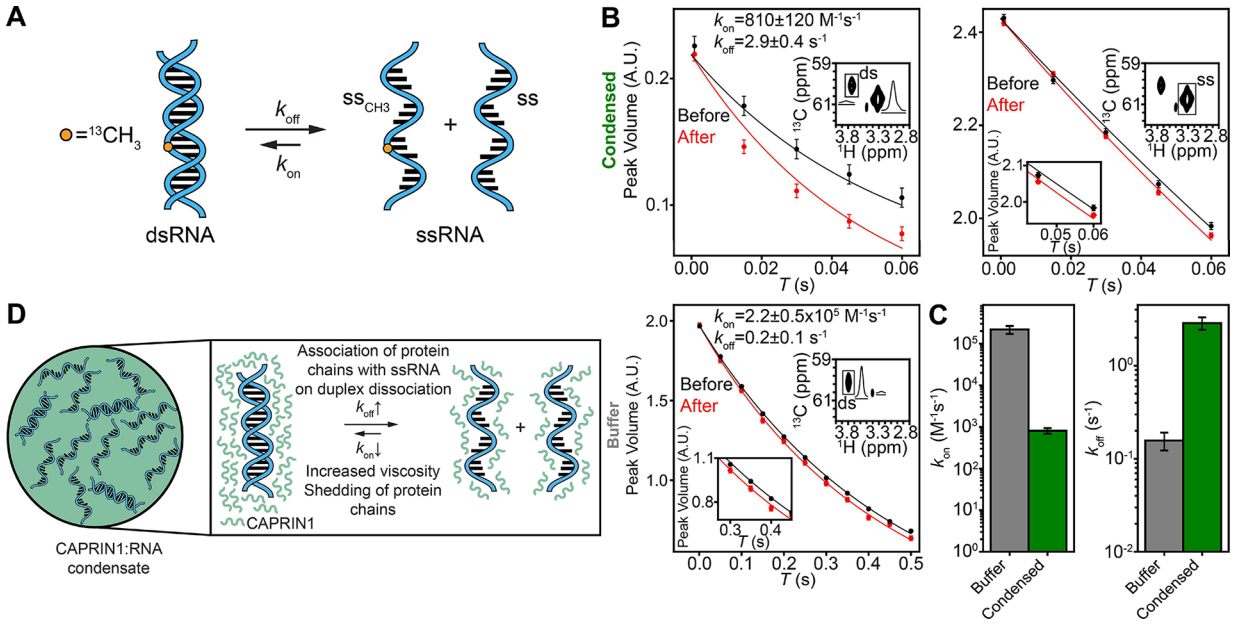

Figure 2. (A) Schematic representation of the dsRNA−ssRNA equilibrium. The 2′-*O*-methyl group probe is denoted by an orange circle. (B) Intensities of diagonal peaks as a function of mixing time, *T*, for dsRNA (top, left) and ssRNA (top, right) in the condensed phase and for dsRNA in buffer (bottom, left) as measured via magnetization exchange experiments where the exchange block is placed either before (black) or after (red) carbon chemical shift evolution (Figure S5, Supporting Information). Error bars were obtained from duplicate experiments; the solid line is a fit to the data to extract kinetic parameters for duplex hybridization. Shown in insets are ddHMQC spectra with intensities from boxed peaks plotted in the main panel, with 1D slices along the ^{1}H dimension (top right of main panel). Also shown in insets are zoomed-in regions of the data (bottom left of main panel). Only data from dsRNA are plotted for buffer, as the ssRNA peak is weak and intensities are unreliable (Supporting Information). Measurements were performed at 57.5 °C, 800 MHz. (C) Bar plots comparing on- and off-rates for duplex hybridization of RNA in buffer (gray) and in CAPRIN1 condensed phase (green). (D) Schematic depicting destabilization of dsRNA in CAPRIN1 condensed phase via an increase (decrease) in k_{off} (k_{on}). Errors for the fitted exchange rates (B and C) were obtained using a Monte Carlo procedure (Supporting Information). The RNA concentration was 100 μM (950 μM) for each strand for measurements in buffer (condensate).

fold increase in off-rate could be due to rapid association of CAPRIN1 with ssRNA as it dissociates from the duplex, ensuring that reassociation of proximal RNA chains to reform dsRNA does not occur (Figure 2D) or from interactions between CAPRIN1 and regions of the dsRNA that begin to melt, which similarly promote formation of ssRNA.

Our results suggest an important role for phase separation whereby the proteinaceous condensate scaffold contributes solvent interactions that modulate molecular recognition processes, such as RNA hybridization in this case. Given the high concentration of CAPRIN1 in the condensed phase (19.1 ± 1.5 mM or 211 ± 16 mg/mL, 40 °C), only 3-fold less than the concentration of water (~688 ± 5 mg/mL; 40 °C) (Supporting Information), CAPRIN1 can be thought of as a solvent, affecting the conformational equilibria of[19] and interactions between[20] client molecules, to control biological function.

■ ASSOCIATED CONTENT

Supporting Information

The Supporting Information is available free of charge at https://pubs.acs.org/doi/10.1021/jacs.4c06530.

Protein/RNA sample preparation, NMR experimental procedures, and data analysis (PDF)

■ AUTHOR INFORMATION

Corresponding Authors

Atul K. Rangadurai − *Department of Molecular Genetics, University of Toronto, Toronto, ON M5S 1A8, Canada; Department of Chemistry, University of Toronto, Toronto, ON M5S 3H6, Canada; Department of Biochemistry, University of Toronto, Toronto, ON M5S 1A8, Canada; Program in Molecular Medicine, Hospital for Sick Children Research Institute, Toronto, ON M5G 0A4, Canada;* Email: rala.atulk@gmail.com

Lewis E. Kay − *Program in Molecular Medicine, Hospital for Sick Children Research Institute, Toronto, ON M5G 0A4, Canada; Department of Molecular Genetics, University of Toronto, Toronto, ON M5S 1A8, Canada; Department of Chemistry, University of Toronto, Toronto, ON M5S 3H6, Canada; Department of Biochemistry, University of Toronto, Toronto, ON M5S 1A8, Canada;* orcid.org/0000-0002-4054-4083; Email: lewis.kay@utoronto.ca

Authors

Lisa Ruetz − *Institute of Organic Chemistry and Center for Molecular Biosciences Innsbruck (CMBI), University of Innsbruck, 6020 Innsbruck, Austria*

Rashik Ahmed − *Department of Molecular Genetics, University of Toronto, Toronto, ON M5S 1A8, Canada; Department of Chemistry, University of Toronto, Toronto, ON M5S 3H6, Canada; Department of Biochemistry, University of Toronto, Toronto, ON M5S 1A8, Canada; Program in Molecular Medicine, Hospital for Sick Children Research Institute, Toronto, ON M5G 0A4, Canada*

Kristen Lo − *Department of Biochemistry, University of Toronto, Toronto, ON M5S 1A8, Canada*

Martin Tollinger − *Institute of Organic Chemistry and Center for Molecular Biosciences Innsbruck (CMBI), University of*

Innsbruck, 6020 Innsbruck, Austria; orcid.org/0000-0002-2177-983X

Julie D. Forman-Kay − *Department of Biochemistry, University of Toronto, Toronto, ON M5S 1A8, Canada; Program in Molecular Medicine, Hospital for Sick Children Research Institute, Toronto, ON M5G 0A4, Canada;* orcid.org/0000-0001-8265-972X

Christoph Kreutz − *Institute of Organic Chemistry and Center for Molecular Biosciences Innsbruck (CMBI), University of Innsbruck, 6020 Innsbruck, Austria;* orcid.org/0000-0002-7018-9326

Complete contact information is available at: https://pubs.acs.org/10.1021/jacs.4c06530

Funding

L.E.K. was funded by the Canadian Institutes of Health Research (FND-503573) and the Natural Sciences and Engineering Council of Canada (2015-04347). This research was funded in part by the Austrian Science Fund (FWF) [10.55776/I5287, 10.55776/F80, 10.55776/P33953] and further supported by the Austrian Research Promotion Agency FFG (West-Austrian BioNMR, 858017).

Notes

The authors declare no competing financial interest.

■ ACKNOWLEDGMENTS

R.A. and A.K.R. acknowledge postdoctoral support from the CIHR.

■ REFERENCES

(1) Banani, S. F.; Lee, H. O.; Hyman, A. A.; Rosen, M. K. Biomolecular condensates: organizers of cellular biochemistry. *Nat. Rev. Mol. Cell Biol.* **2017**, *18* (5), 285−298.

(2) Ripin, N.; Parker, R. Formation, function, and pathology of RNP granules. *Cell* **2023**, *186* (22), 4737−4756.

(3) Nam, J.; Gwon, Y. Neuronal biomolecular condensates and their implications in neurodegenerative diseases. *Front Aging Neurosci* **2023**, *15*, 1145420.

(4) Tsang, B.; Pritisanac, I.; Scherer, S. W.; Moses, A. M.; Forman-Kay, J. D. Phase Separation as a Missing Mechanism for Interpretation of Disease Mutations. *Cell* **2020**, *183* (7), 1742−1756.

(5) Langdon, E. M.; Qiu, Y.; Ghanbari Niaki, A.; McLaughlin, G. A.; Weidmann, C. A.; Gerbich, T. M.; Smith, J. A.; Crutchley, J. M.; Termini, C. M.; Weeks, K. M.; Myong, S.; Gladfelter, A. S. mRNA structure determines specificity of a polyQ-driven phase separation. *Science* **2018**, *360* (6391), 922−927.

(6) Cakmak, F. P.; Choi, S.; Meyer, M. O.; Bevilacqua, P. C.; Keating, C. D. Prebiotically-relevant low polyion multivalency can improve functionality of membraneless compartments. *Nat. Commun.* **2020**, *11* (1), 5949.

(7) Nott, T. J.; Craggs, T. D.; Baldwin, A. J. Membraneless organelles can melt nucleic acid duplexes and act as biomolecular filters. *Nat. Chem.* **2016**, *8* (6), 569−75.

(8) Iglesias-Artola, J. M.; Drobot, B.; Kar, M.; Fritsch, A. W.; Mutschler, H.; Dora Tang, T. Y.; Kreysing, M. Charge-density reduction promotes ribozyme activity in RNA-peptide coacervates via RNA fluidization and magnesium partitioning. *Nat. Chem.* **2022**, *14* (4), 407−416.

(9) Ahmed, R.; Rangadurai, A. K.; Ruetz, L.; Tollinger, M.; Kreutz, C.; Kay, L. E. A delayed decoupling methyl-TROSY pulse sequence for atomic resolution studies of folded proteins and RNAs in condensates. *J. Magn. Reson.* **2024**, *362*, 107667.

(10) Rosenzweig, R.; Kay, L. E. Bringing dynamic molecular machines into focus by methyl-TROSY NMR. *Annu. Rev. Biochem.* **2014**, *83*, 291−315.

(11) Ayadi, L.; Galvanin, A.; Pichot, F.; Marchand, V.; Motorin, Y. RNA ribose methylation (2'-O-methylation): Occurrence, biosynthesis and biological functions. *Biochim Biophys Acta Gene Regul Mech* **2019**, *1862* (3), 253−269.

(12) Kumar, S.; Mapa, K.; Maiti, S. Understanding the effect of locked nucleic acid and 2'-O-methyl modification on the hybridization thermodynamics of a miRNA-mRNA pair in the presence and absence of AfPiwi protein. *Biochemistry* **2014**, *53* (10), 1607−15.

(13) Nakayama, K.; Ohashi, R.; Shinoda, Y.; Yamazaki, M.; Abe, M.; Fujikawa, A.; Shigenobu, S.; Futatsugi, A.; Noda, M.; Mikoshiba, K.; Furuichi, T.; Sakimura, K.; Shiina, N. RNG105/caprin1, an RNA granule protein for dendritic mRNA localization, is essential for long-term memory formation. *Elife* **2017**, *6*, No. e29677.

(14) Youn, J. Y.; Dunham, W. H.; Hong, S. J.; Knight, J. D. R.; Bashkurov, M.; Chen, G. I.; Bagci, H.; Rathod, B.; MacLeod, G.; Eng, S. W. M.; Angers, S.; Morris, Q.; Fabian, M.; Cote, J. F.; Gingras, A. C. High-Density Proximity Mapping Reveals the Subcellular Organization of mRNA-Associated Granules and Bodies. *Mol. Cell* **2018**, *69* (3), 517−532.

(15) Kloiber, K.; Spitzer, R.; Tollinger, M.; Konrat, R.; Kreutz, C. Probing RNA dynamics via longitudinal exchange and CPMG relaxation dispersion NMR spectroscopy using a sensitive 13C-methyl label. *Nucleic Acids Res.* **2011**, *39* (10), 4340−51.

(16) Tugarinov, V.; Hwang, P. M.; Ollerenshaw, J. E.; Kay, L. E. Cross-correlated relaxation enhanced 1H[bond]13C NMR spectroscopy of methyl groups in very high molecular weight proteins and protein complexes. *J. Am. Chem. Soc.* **2003**, *125* (34), 10420−8.

(17) Farrow, N. A.; Zhang, O.; Forman-Kay, J. D.; Kay, L. E. A heteronuclear correlation experiment for simultaneous determination of 15N longitudinal decay and chemical exchange rates of systems in slow equilibrium. *J. Biomol NMR* **1994**, *4* (5), 727−34.

(18) Craig, M. E.; Crothers, D. M.; Doty, P. Relaxation kinetics of dimer formation by self complementary oligonucleotides. *J. Mol. Biol.* **1971**, *62* (2), 383−401.

(19) Tibble, R. W.; Gross, J. D. A call to order: Examining structured domains in biomolecular condensates. *J. Magn. Reson.* **2023**, *346*, 107318.

(20) de Vries, T.; Novakovic, M.; Ni, Y.; Smok, I.; Inghelram, C.; Bikaki, M.; Sarnowski, C. P.; Han, Y.; Emmanouilidis, L.; Padroni, G.; Leitner, A.; Allain, F. H. Specific protein-RNA interactions are mostly preserved in biomolecular condensates. *Sci. Adv.* **2024**, *10* (10), No. eadm7435.